



CHORUS

This is the accepted manuscript made available via CHORUS. The article has been published as:

## Rotator-to-Lamellar Phase Transition in Janus Colloids Driven by Pressure Anisotropy

Hossein Rezvantalab, Daniel J. Beltran-Villegas, and Ronald G. Larson

Phys. Rev. Lett. **117**, 128001 — Published 16 September 2016

DOI: [10.1103/PhysRevLett.117.128001](https://doi.org/10.1103/PhysRevLett.117.128001)

# Rotator-to-Lamellar Phase Transition in Janus Colloids Driven by Pressure Anisotropy

Hossein Rezvantalab, Daniel J. Beltran-Villegas, and Ronald G. Larson

*Department of Chemical Engineering, University of Michigan, Ann Arbor, Michigan, 48109, USA*

**Abstract-** We demonstrate through Brownian dynamics simulations a phase transition in plastic crystalline assemblies of Janus spheres through controlled pressure anisotropy. When the pressure in plane with hexagonally ordered layers is increased relative to that normal to the layers, a rapid first-order rotator-to-lamellar transition of Janus sphere orientation occurs at constant temperature. We show that the underlying mechanism closely follows the Maier-Saupe theory, originally developed for isotropic-to-nematic transition in positionally disordered materials but here applied to positionally ordered ones. Since the transition involves almost no translational diffusion or volume change, and occurs rapidly by particle rotation, the results should help guide the design of rapidly switchable colloidal crystals.

Self-assembly of colloidal particles is a promising way to develop new materials with targeted properties. The large freedom in control over the inter-particle potential has made it possible to design colloidal particles which significantly extend the possibilities offered by atomic systems [1, 2]. Such particles form colloidal crystals, structures analogous to molecular crystals with long-range order and characteristic length on the order of particle size [3, 4]. The possibility of controlling and reconfiguring such crystals is attractive for many technological applications. An example is the ability of such structures to manipulate light with wavelengths in the visible range set by particle size and packing periodicity [5], with applications in wave guides, band pass filters, and negative refractive index materials [6, 7]. Designing processes that enable the formation of such novel materials requires thorough understanding of the equilibrium

thermodynamics of crystal formation and the kinetics of their formation and reconfiguration.

One of the most interesting features of colloidal particles is the possibility of tuning and patterning their surface chemistry. Due to recent advances in particle synthesis methods [8, 9], it is now possible to fabricate particles decorated with patches of well-defined number, size, and geometrical arrangement [10, 11]. The most elementary and geometrically simple surface-patterned particle is a Janus sphere, characterized by a surface divided into two regions of differing chemical composition [12]. While using homogeneous spheres as building blocks for colloidal crystals typically yields close-packed structures with slight room for variability [13], Janus spheres can spontaneously self-assemble into a variety of structures, holding promise for development of materials with novel functional, mechanical, and optical properties. Some of the structures realized so far include clusters, helices, and worm-like aggregates [14-16].

Most of the available equilibrium phase behavior studies on single-patch Janus particles have focused on the square-well Kern-Frenkel type potential typically parameterized to represent long-range interactions, *i.e.* those enabling a fluid-fluid phase separation [17-20]. These studies revealed the spontaneous formation of micelles, lamellae, tubes, wrinkled sheets, and other close-packed structures with varying degrees of orientational order. Smooth and shorter-ranged potentials have been considered in a few recent works [21, 22] providing more realistic interactions comparable with traditional colloidal forces. The important parameters governing the phase behavior of Janus spheres are considered to be: the volume fraction, surface coverage of the attractive cap, temperature non-dimensionalized by the interaction strength, and the interaction range normalized by particle size, with the pressure presumably set by the volume fraction. However, the broken symmetry in surface coverage causes the pressure to generally depend on the orientational distribution of neighboring particles, which can vary along different directions. This so-far-overlooked possibility adds another dimension to characterization of phase behavior in systems comprised of anisotropic particles. A particularly attractive prospect is to make colloidal assemblies that can be switched from one structure to another through controlled pressure anisotropy.

In this Letter, we show using Janus building blocks that tuning the ratio of lateral to normal pressures can trigger a transition between two solid phases: from an isotropic crystal with orientational disorder (*i.e.* a rotator phase) to an orientationally ordered crystal with lamellae in the desired direction. In contrast to the phases shown in previous studies, we develop phase diagrams based on the new dimension of pressure anisotropy and discuss the physical mechanism governing the observed solid-solid transition. The novelty and significance of the proposed mechanism lies in the fact that it does not require tuning the particle surface or interaction strength, which would experimentally require involved fabrication procedures or fine control over size, shape, and concentration of introduced depletants/linkers. Furthermore, we demonstrate that this tunable orientational ordering can be explained semi-quantitatively in terms of the Maier-Saupe theory for an isotropic-nematic phase transition, where a phenomenological energy constant can be parameterized in terms of the chemical patchiness, interaction strength, and the applied pressures and temperature. The theoretical analysis helps in generalizing the observed transition, which can provide crucial insight in designing switchable and reconfigurable materials for targeted applications.

We consider Janus spheres comprised of an attractive cap whose size is characterized by the central half-angle  $\alpha$  known as the Janus balance [22], and a repulsive cap covering the rest of the surface ( $2\pi - 2\alpha$ ). To model the anisotropic interaction between these particles, we use a functional form similar to the one proposed by Miller and Cacciuto [21], expressing the potential between particles  $i$  and  $j$  as

$$u(r_{ij}, \theta_i, \theta_j) = u_{SLJ}(r_{ij}) + f(\theta_i)f(\theta_j)u_M(r_{ij}) \quad (1)$$

where  $r_{ij}$  is the distance between the centers of the two particles,  $\theta_i$  is the angle between the director of particle  $i$  and the center-to-center vector connecting particles  $i$  and  $j$ ,  $u_{SLJ}$  is a short-range repulsive potential that follows a shifted Lennard-Jones form,  $u_M$  is an attractive Morse potential, and  $f(\theta)$  is an orientation-dependent factor which is unity when  $\theta < \alpha$  and rapidly but smoothly decays to zero when  $\theta$  crosses the edge of Janus boundary. The overall potential is proportional to an interaction parameter  $\varepsilon$ . We use the thermal energy  $k_B T = 1$  as the unit of energy, the particle diameter  $\sigma = 1$  as the unit of length, and the particle mass  $m = 1$  as the mass unit in our calculations, with the time scale

derived using these choices of scaling as  $\tau = \sigma \sqrt{m/k_B T}$ . Details of the interaction potential and parameters can be found elsewhere [22].

In order to demonstrate the role of pressure anisotropy in governing the phase behavior, we employ a modified version of Martyna-Tobias-Klein's NPT integrator which allows independent box length fluctuations along three coordinate axes [23]. This fully flexible cell method—which solves the coupled equations of motion for the thermostat and barostat—allows us to specify independent target pressures along different directions. Brownian dynamics simulations are performed on systems comprised of 1440 colloidal particles with periodic boundaries, starting from an initial FCC lattice and allowing sufficient time for equilibration under given pressures. We take the lateral pressures  $p_{xx} = p_{yy}$  to be different from the normal one  $p_{zz}$ , and investigate the phase behavior under various sets of pressures while fixing the Janus balance  $\alpha$  and interaction strength  $\varepsilon$ . The simulations are repeated with doubled domain size as well as using different starting configurations to confirm the final equilibrium structures are not an artifact of the number of particles or the initial state.

To quantify the orientational order, we use the order parameter  $\langle P_2 \rangle$  obtained by an ensemble average over the second Legendre polynomial for the particle pair orientation

$$\langle P_2 \rangle = \left\langle \frac{3}{N_i} \sum_{j=1}^{N_i} (\mathbf{u}_i \cdot \mathbf{u}_j)^2 - 1 \right\rangle / 2 \quad (2)$$

where  $N_i$  is the number of near neighbors of particle  $i$  lying within the potential cutoff,  $\mathbf{u}_i$  is the unit vector from the center of particle  $i$  directed to the center of its attractive cap, and the brackets  $\langle \dots \rangle$  represent averaging over all particles  $i$  in the system [24]. If  $\langle P_2 \rangle \approx 0$ , a rotator close-packed structure is formed with positional order but random orientations of the attractive caps, while higher values (taken here as  $\langle P_2 \rangle > 0.3$ ) correspond to a lamellar structure with both crystalline and orientational order in which particles form bilayers with attractive caps facing each other.

Figure 1 shows the variation of pressure components  $p_{xx}$ ,  $p_{yy}$ ,  $p_{zz}$ , volume fraction  $\phi$ , mean inter-particle separations  $\lambda_x$ ,  $\lambda_y$ ,  $\lambda_z$ , and the order parameter  $\langle P_2 \rangle$  for two different ratios of lateral to normal pressure. The particles are characterized by an attractive cap of  $\alpha = 117^\circ$  (shown in blue in the snapshots) and an interaction strength of  $\varepsilon/k_B T = 1.05$ ,

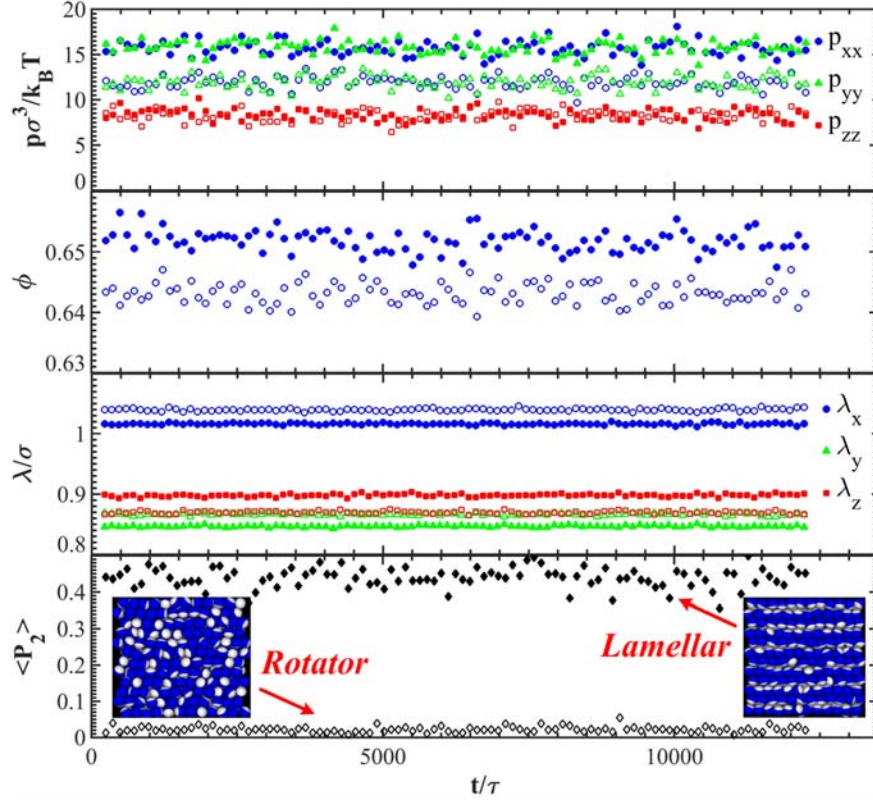


FIG. 1 Temporal variation of pressure components  $p$ , volume fraction  $\phi$ , mean inter-particle separation  $\lambda$  in three directions, and orientational order parameter  $\langle P_2 \rangle$  along with equilibrated renderings, for a system of Janus colloids with  $\alpha = 117^\circ$ ,  $\epsilon/k_B T = 1.05$  subject to two different anisotropic pressure conditions:  $p_{zz} = 8 k_B T/\sigma^3$ , and  $p_{xx} = p_{yy} = 12$  (open symbols) or  $p_{xx} = p_{yy} = 16$  (filled symbols).

and the normal pressure is set to  $p_{zz} = 8k_B T/\sigma^3$  in both cases. We note that the pressures quickly approach the set values and fluctuate by  $<10\%$ . The temperature also corresponded to the set value ( $k_B T = 1$ ) with limited fluctuations (not shown). Increasing the lateral pressure from  $p_{xx} = p_{yy} = 12k_B T/\sigma^3$  to 16 results in  $\sim 1.4\%$  increase in volume fraction, which can also be realized from the increased overall inter-particle separations. On the other hand, the order parameter  $\langle P_2 \rangle$  and equilibrium renderings show a phase transition from rotator to lamellar upon lateral compression. Note that the system retains the FCC positional order in both phases, yielding equal numbers of crystalline neighbors [22].

To evaluate the nature of this transition and determine phase boundaries, we systematically tune the lateral and normal pressures for each particle/interaction type. Finding the phase at each state point requires simulating a large system for more than  $10^8$

time steps to ensure sufficient statistics for evaluating the thermodynamic properties, which is done with GPUs using the Highly Optimized Object-Oriented Molecular Dynamics package (HOOMD) [25]. To improve the efficiency, we fix the pressure ratio  $p_{xx}/p_{zz}$  for any given  $\alpha$  and  $\varepsilon$ , and ramp down the two pressures simultaneously to cover the desired range of normal pressure. The result is shown in Fig. 2(a) for the above particles subject to a pressure ratio of  $p_{xx}/p_{zz} = 2$ . Note that the ramping is done slowly enough that the system remains close to equilibrium at any point during the pressure reduction. To confirm this, we varied the rate of ramping for selected cases, and also verified a match with the properties found from long constant-pressure simulations as in Fig. 1. The phase behavior was also found to be reversible irrespective of the direction of pressure ramping (see Supplemental Material [26]). We can see that upon reaching a normal pressure of  $p_{zz} = 6.5k_B T/\sigma^3$ , the order parameter  $\langle P_2 \rangle$  undergoes a sudden drop. This discontinuity signifies a first-order transition between the two solid phases, from an orientationally-ordered structure to a disordered one. The snapshots indicate that the orientationally-ordered phase is lamellar with the caps oriented along the low-pressure ( $z$ ) direction. When the transition occurs, the mean particle separation along  $z$  drops, meaning that the layers become more closely spaced as they lose orientational order, while  $\lambda_x$ ,  $\lambda_y$  show a sudden jump, corresponding to lateral dilation. The net volume change is negligible as reflected in the nearly continuous variation of volume fraction. Thus the transition involves little movement of the particles but mainly just rotation in place, in response to mechanical actuation. Note that the mean separations along  $x, y$  are not equal since the box dimensions are commensurate with a close-packed hexagonal lattice.

We performed several such simulations while tuning the pressure ratio  $p_{xx}/p_{zz}$  (with  $p_{xx} = p_{yy} = p_{||}$ ), and obtained a phase diagram for the alignment order parameter  $\langle P_2 \rangle$  as a function of pressures. This is shown in Fig. 2(b) by color-coding  $\langle P_2 \rangle$  for the above case of  $\alpha = 117^\circ$ ,  $\varepsilon/k_B T = 1.05$  along with that for a higher interaction strength of  $\varepsilon/k_B T = 1.20$ . While application of an isotropic pressure does not induce orientational order in the solid phase, one can see a clear transition to a lamellar phase when  $p_{xx} = p_{yy} > p_{zz}$  and the pressures are sufficiently high. The higher the pressure anisotropy, the lower the minimum normal pressure  $p_{zz}$  required to trigger the formation of lamellae. Note that at

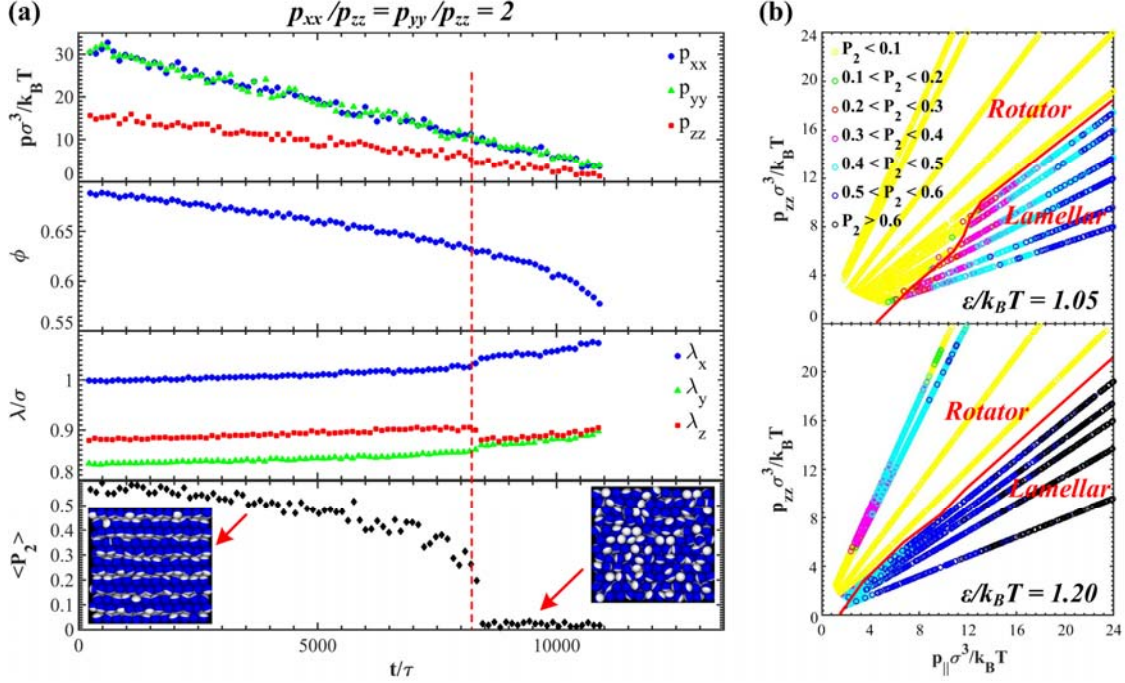


**FIG. 2** (a) Variation of pressure components, volume fraction, mean inter-particle separations, and orientational order parameter for a system of Janus colloids with  $\alpha = 117^\circ$ ,  $\epsilon/k_B T = 1.05$  subject to a constant lateral/normal pressure ratio of 2 while reducing pressure magnitude over time; (b) phase diagrams of color-coded order parameter as a function of applied pressures for particles with  $\alpha = 117^\circ$  and two different interaction strengths.

the lower-left corner of the phase plane, a fluid phase will be formed only under isotropic pressure conditions. Furthermore, increasing the interaction strength to  $\epsilon/k_B T = 1.20$  extends the lamellar region in the phase plane as the attractive caps have a higher tendency to align under similar pressures. We also note that on the left side of the phase diagram where  $p_{xx} = p_{yy} < p_{zz}$ , a weakly-lamellar phase starts to form at the higher interaction strength,  $\epsilon/k_B T = 1.20$ . For this reversed pressure anisotropy, there are two low-pressure directions that compete to direct the orientation of the lamellae. We find that a pressure along the axisymmetry axis that is higher than that along the lateral directions can cause the lamellae to buckle, leading to a defective structure. Therefore, the maximum orientational order can be achieved by imposing a higher pressure along the two lateral directions than along the axisymmetry axis. This mechanically-actuated phase transition might have potential implications in designing novel materials *e.g.* tunable optical devices: an isotropic material with a white noise response to optical

signals can be transformed into one with distinct response along two perpendicular axes upon imposing the proper pressure anisotropy.

For all of the structures formed, we also quantify the director order parameter defined by [27]

$$S = (3/2 \mathbf{S} : \mathbf{S})^{1/2}, \quad \mathbf{S} = \langle \mathbf{u} \mathbf{u} - 1/3 \boldsymbol{\delta} \rangle \quad (3)$$

where  $\boldsymbol{\delta}$  is the unit tensor, and  $\mathbf{u}$  is the orientation vector of the Janus cap for each particle with respect to a director taken here as the  $z$ -axis. The variation of  $S$  with the normal pressure is shown in Fig. 3(a) for  $\alpha = 117^\circ$ ,  $\varepsilon/k_B T = 1.05$ , and different pressure ratios  $p_{xx}/p_{zz}$ . In all cases, the order parameter jumps from nearly zero to  $S^* = 0.43 \pm 0.04$  at the transition. The value of  $S^*$  is obtained by fitting a straight line to the order parameter in the rotator phase  $S_R(t)$  and a fifth-order polynomial to that of the lamellar region  $S_L(t)$ , and splicing them with a sigmoidal function,  $\Xi(t) = (1 + \exp[(t-t^*)/C])^{-1}$ , as  $S(t) = S_R(t) + \Xi(t) (S_L(t) - S_R(t))$ , leading to the order parameter at the transition as  $S^* = S_L(t^*)$ . The universal jump to  $S^* \approx 0.43$  is characteristic of a Maier-Saupe (M-S) like transition which explains qualitatively the isotropic-to-nematic phase transition in thermotropic melts. The

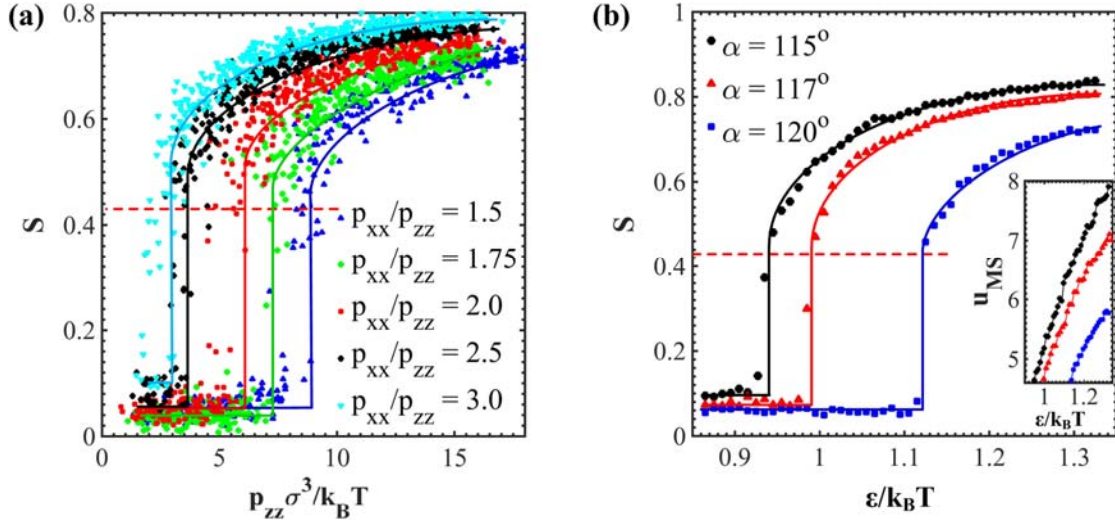


FIG. 3 (a) Director order parameter  $S$  as a function of normal pressure  $p_{zz}$  for Janus colloids with  $\alpha = 117^\circ$ ,  $\varepsilon/k_B T = 1.05$  subject to several lateral/normal pressure ratios, with the dashed red line indicating the order parameter at the transition according to the Maier-Saupe theory; (b) variation of  $S$  with  $\varepsilon$  for colloids with different Janus balance subject to fixed pressures of  $p_{xx} = p_{yy} = 16$ ,  $p_{zz} = 8 k_B T/\sigma^3$ ; solid lines are polynomial-linear fits connected by a sigmoidal function. The inset shows variation of Maier-Saupe parameter  $u_{MS}$  with  $\varepsilon$  within the lamellar region.

M-S theory takes into account only orientational entropy and anisotropic energetic contribution, but no anisotropic shape-packing effects [28], and is therefore an inadequate model for most nematic liquid crystals, which are composed of molecules with large shape anisotropy, typically rod-like. However, we find that the M-S theory is a good model for our system, which is composed of geometrically isotropic spheres for which the tendency to orient is entirely due to the anisotropic Janus interactions and not at all due to shape anisotropy.

To show the universality of this transition, we also evaluate the phase behavior while tuning the size of the attractive cap  $\alpha$  and the interaction strength  $\varepsilon$  at constant imposed pressures of  $p_{xx} = p_{yy} = 16$ ,  $p_{zz} = 8 k_B T / \sigma^3$ . Figure 3(b) suggests a similar jump in  $S$  at transition for multiple values of Janus balance. It should be noted that the narrow range of  $\alpha$  explored here is intended to localize the transition within the window of modest  $\varepsilon/k_B T = 0.8-1.4$ ; the physics is similar for particles with smaller/larger Janus balance, but with the transition shifted to lower/higher interaction strengths. On the other hand, the phase diagram for any given attractive cap size  $\alpha$  is generally similar to the ones shown in Fig. 2(b), only with the lamellar region shifted to larger pressures upon increasing  $\alpha$ .

The Maier-Saupe potential is generally expressed as [27]

$$V_{MS}(\mathbf{u}) = \text{const} - 3/2 u_{MS} \mathbf{u} \mathbf{u} : \mathbf{S} \quad (4)$$

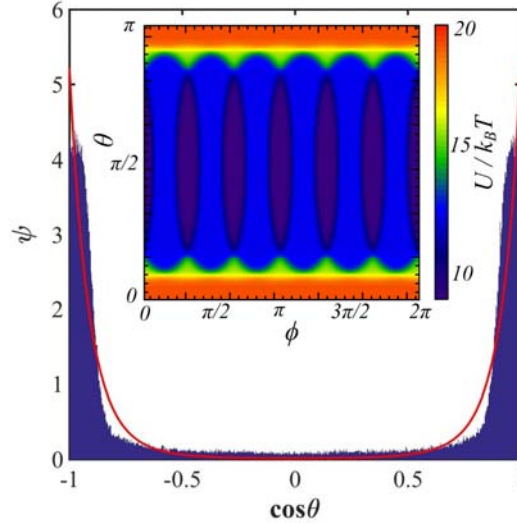
where  $u_{MS}$  is a phenomenological energy constant. A one-to-one mapping can be found between the order parameter  $S$  and the M-S interaction strength  $u_{MS}$  at equilibrium [29, 30]. Although this has been shown earlier using a closure approximation, we developed an exact self-consistent solution based on the imaginary error function (see Supplemental Material [26]). Using this mapping, we determined the dependency of  $u_{MS}$  on the interaction strength  $\varepsilon$  for the cases plotted in Fig. 3(b). As shown in the inset,  $u_{MS}$  scales almost linearly with  $\varepsilon$ , which is expected due to the nature of this phenomenological energy constant. Moreover, the transition in all cases appears to occur near  $u_{MS} = 4.55$ , which is the criterion suggested by the M-S theory for isotropic-nematic phase transition. Therefore, single-patch Janus colloids are found to be an excellent model system whose solid-solid phase transition can be explained via the M-S theory. Note that the strength parameter  $u_{MS}$  for the current system can be generally expressed as  $u_{MS}(\alpha, \varepsilon, p_{xx}, p_{zz})$ , where its dependency on pressures can be obtained in a similar way by mapping  $S$  e.g. in

Fig. 3(a) onto  $u_{MS}$ . This universal mapping of all system parameters onto a phenomenological constant governing the order can serve as a promising guideline in designing switchable colloidal crystals for optical and photonic applications [31].

To further evaluate the consistency of the observed phase behavior with the Maier-Saupe theory, we also calculate the probability distribution function of particle orientations and compare it with the theoretical expression obtained by minimizing the free energy using the variational principle as [29]

$$\psi(\mathbf{u}) = C_1 \exp(3/2 S u_{MS} \cos^2 \theta) \quad (5)$$

where the constant  $C_1$  is found using the normalization condition and  $\theta$  is the angle between the orientation vector  $\mathbf{u}$  of the Janus cap and the director. In Fig. 4, this comparison is shown for a system with  $\alpha = 117^\circ$ ,  $\varepsilon/k_B T = 1.05$ ,  $p_{xx} = p_{yy} = 16$ , and  $p_{zz} = 8 k_B T/\sigma^3$ , which yields an ordered phase with  $S \approx 0.55$ . The result (also confirmed for several other values of  $S$ ) indicates reasonable agreement with slight deviation of the simulation data from the M-S theory. The source of discrepancy lies in the hexagonal in-plane positional order of the Janus spheres, which produces a  $60^\circ$  periodicity in the interactions in the azimuthal  $\phi$ -direction. To prove this, we considered a test case scenario of a Janus sphere surrounded by six near neighbors at fixed positions, all with



**FIG. 4** Histogram of the orientation distribution of Janus particles with  $\alpha = 117^\circ$ ,  $\varepsilon/k_B T = 1.05$  simulated under fixed pressures of  $p_{xx} = p_{yy} = 16$ ,  $p_{zz} = 8 k_B T/\sigma^3$ ; the solid red line is the prediction of Maier-Saupe theory from Eq. (5); the inset shows variation of the overall potential in spherical coordinates for an extreme sample case with a rotating central particle.

their attractive caps facing the central particle. The potential was then calculated upon rotating the central particle in  $\theta$ ,  $\varphi$  directions, producing considerable variation along  $\varphi$ , as shown in the insert to Fig. 4. While this example is an extreme one, it shows that the distribution cannot be fully captured with a purely  $\theta$ -dependent function as in Eq. (5).

In conclusion, we have demonstrated a novel phase transition induced by anisotropy in pressure for spherical particles with anisotropic interactions. The key features of this solid-solid plastic crystal first-order transition are that it is induced without adjusting the temperature, volume fraction, or particle surface/interaction strength, and takes place with little translation of the constituent particles. Furthermore, we found that this solid-solid transition bears similarities with the isotropic-nematic liquid-liquid crystalline transition in fluids. To the best of our knowledge, this is the first successful demonstration of the applicability of Maier-Saupe theory to a colloidal phase transition, which allows all significant aspects of the transition to be mapped onto a single pressure and temperature dependent parameter  $u_{MS}$ , paving the way for rapid design and optimization of experimental Janus particle systems in advanced materials.

We acknowledge the support from NSF under grant DMR 1403335 as well as the ARO-MURI program at Army Research Office under grant number 58128MSMUR. The authors are also grateful to the Glotzer Group at University of Michigan for help with using HOOMD-blue simulation package.

## References

- [1] A. Yethiraj, and A. van Blaaderen, *Nature* **421**, 513 (2003).
- [2] S. Sacanna *et al.*, *Nat. Commun.* **4**, 1688 (2013).
- [3] V.N. Manoharan, M.T. Elsesser, and D.J. Pine, *Science* **301**, 483 (2003).
- [4] D. Zerrouki *et al.*, *Langmuir* **22**, 57 (2006).
- [5] J.D. Joannopoulos *et al.*, *Photonic crystals: molding the flow of light* (Princeton university press, 2011).
- [6] A. Mekis *et al.*, *Phys. Rev. Lett.* **77**, 3787 (1996).
- [7] D.R. Smith, J.B. Pendry, and M.C.K. Wiltshire, *Science* **305**, 788 (2004).
- [8] A. Walther, and A.H.E. Mueller, *Chem. Rev.* **113**, 5194 (2013).
- [9] G. Loget, and A. Kuhn, *J. Mater. Chem.* **22**, 15457 (2012).

- [10] A.B. Pawar, and I. Kretzschmar, *Macromolecular Rapid Communications* **31**, (2010).
- [11] Q. Chen *et al.*, *Langmuir* **28**, (2012).
- [12] H. Rezvantalab, and S. Shojaei-Zadeh, *Soft Matter* **9**, 3640 (2013).
- [13] J. Zhang *et al.*, *Appl. Phys. Lett.* **81**, 3176 (2002).
- [14] Q. Chen *et al.*, *Science* **331**, 199 (2011).
- [15] M.S. Fernandez, V.R. Misko, and F.M. Peeters, *Phys. Rev. E* **92**, 042309 (2015).
- [16] Q.-Z. Zou *et al.*, *Nanoscale* **8**, 4070 (2016).
- [17] F. Sciortino, A. Giacometti, and G. Pastore, *Phys. Rev. Lett.* **103**, 237801 (2009).
- [18] F. Sciortino, A. Giacometti, and G. Pastore, *Phys. Chem. Chem. Phys.* **12**, 11869 (2010).
- [19] Z. Preisler *et al.*, *J. Phys. Chem. B* **117**, 9540 (2013).
- [20] T. Vissers *et al.*, *J. Chem. Phys.* **138**, 164505 (2013).
- [21] W.L. Miller, and A. Cacciuto, *Phys. Rev. E* **80**, 021404 (2009).
- [22] D.J. Beltran-Villegas *et al.*, *Soft Matter* **10**, 4593 (2014).
- [23] T.-Q. Yu *et al.*, *Chem. Phys.* **370**, 294 (2010).
- [24] P.R. tenWolde, M.J. RuizMontero, and D. Frenkel, *J. Chem. Phys.* **104**, 9932 (1996).
- [25] J.A. Anderson, C.D. Lorenz, and A. Travesset, *J. Comput. Phys.* **227**, 5342 (2008).
- [26] See Supplemental Material for simulation validation tests and derivation of the exact mapping between  $S$  and  $u_{MS}$ .
- [27] R.G. Larson, *The Structure and Rheology of Complex Fluids* (Oxford University Press, New York, 1999).
- [28] R.G. Larson, *Constitutive Equations for Polymer Melts and Solutions* (Butterworth-Heinemann, Stoneham, 1988).
- [29] P.G. de Gennes, and J. Prost, *The physics of liquid crystals*, Clarendon. 1993, Oxford.
- [30] M. Doi, and S.F. Edwards, *The theory of polymer dynamics* (oxford university press, 1988).
- [31] S.-H. Kim *et al.*, *NPG Asia Mater.* **3**, 25 (2011).